ISBN: 978-3-95450-132-8 doi:10.18429/JACoW-IPAC2014-TUPRI101

MEASUREMENT OF NEUTRONS GENERATED BY 345 MeV/u U-238 BEAM AT RIKEN RIBF

Noriaki Nakao#, Institute of Technology, Shimizu Corporation, Tokyo, Japan
Yoshitomo Uwamino, RIKEN, Wako, Saitama, Japan
Kanenobu Tanaka, RIKEN, Wako, Saitama, Japan

Abstract

Neutrons generated by 345 MeV/u uranium beam bombardment on a 3-mm-thick beryllium target were measured outside the target chamber using activation detectors of bismuth, aluminum and carbon at 60, 70 and 90 degrees from the beam axis. Following several days of irradiation and photo peak analyses, the production rates of the radionuclides were obtained for the reactions of ^{209}Bi(n,xn)$^{210-x}$Bi(x=4-10), ^{12}C(n,2n)^{11}C and ^{27}Al(n,α)^{24}Na.

A PHITS Monte Carlo simulation for production rates was performed and comparisons with the measurements showed good agreements to within approximately 60%.

INTRODUCTION

Currently, a number of high-power accelerators to be used in radioisotope beam facilities are under construction. With regard to radiation safety in these facilities, secondary neutron data due to beam irradiation is very important for predicting the levels of activation and prompt radiation. Neutron energy spectra in the forward direction from an iron target measured in GSI [1] are available for a 1GeV/u ^{238}U beam. However, experimental data for secondary neutrons produced by a uranium beam is very scarce. Since 2007, the Radioactive Isotope Beam Factory (RIBF) at RIKEN has supplied uranium beams at energies of approximately 350 MeV/u to a target in the big RIKEN projectile-fragment separator (BigRIPS)[2].

Activation detectors are useful for measuring radiation fields in narrow regions or gaps in actual accelerator facilities. In a previous measurement [3], neutron and photon distributions around the BigRIPS separator were measured for a uranium beam using activation detectors and thermoluminescent dosimeters (TLD). To obtain benchmark experimental data for secondary neutrons produced by a target impacted with a uranium beam, the present study was performed using activation detectors placed at several locations just outside the target chamber.

EXPERIMENT

Figures 1 and 2 show the experimental setup at the aluminum F0 chamber in the BigRIPS. The F0 target (3-mm-thick Be), which is equipped inside the chamber, is injected with 345 MeV/u uranium beam. The generated radioisotopes (RIs) and the penetrating uranium beam at a forward angle pass through the hole of a copper scraper and are transported downstream as indicated in the figures.

Neutron measurements using the activation detectors were performed parasitically with the RI beam experiments. To measure secondary neutrons from the F0 target, the activation detector samples of bismuth (20-mmϕ×2-mm), aluminum (20-mmϕ×2-mm) and graphite (40-mmϕ×4-mm) were placed outside of the chamber at angles of 60, 70 and 90 degrees from the target point and from the beam line as shown in Fig. 1. In the case of 60 degrees, two locations at the 'side' and 'under' the beam line were employed. The samples at 60 and 70 degrees were placed between the F0 chamber and stainless steel shield in the forward direction, and the samples at 90 degrees were placed on the glass of the viewport window. The average intensity of the uranium beam for the 2.5-day irradiation period was approximately 5×10^{10} sec^{-1} (~8 particle nano amperes) with a 20% uncertainty.

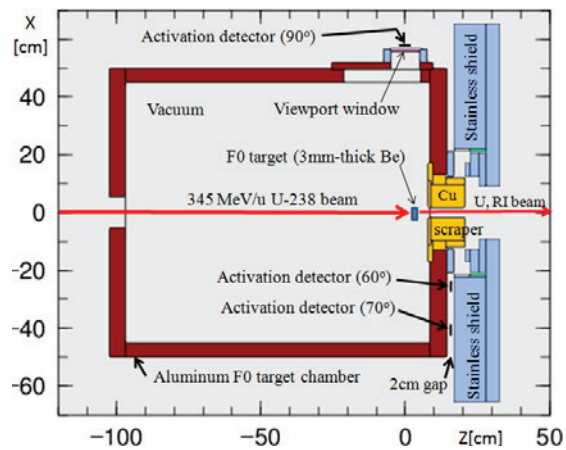

Figure 1: Horizontal cross-section of the target chamber.

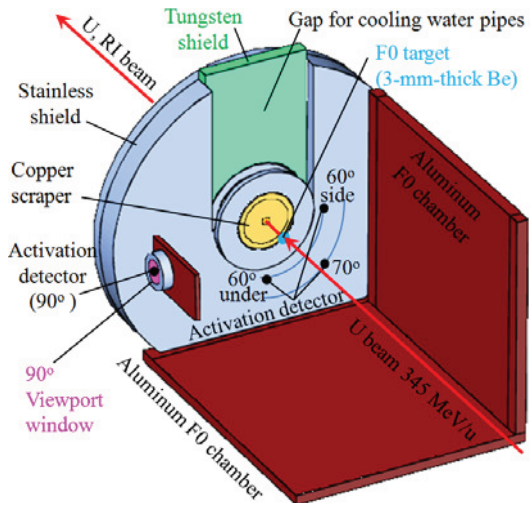

Figure 2: Three dimensional bird's-eye-view removing some chamber walls to see the detector sample positions.

#noriaki.nakao@shimz.co.jp

Content from this work may be used under the terms of the CC BY 3.0 licence (© 2014). Any distribution of this work must maintain attribution to the author(s), title of the work, publisher, and DOI.

ISBN: 978-3-95450-132-8 doi:10.18429/JACoW-IPAC2014-TUPRI101

Content from this work may be used under the terms of the CC BY 3.0 licence (© 2014). Any distribution of this work must maintain attribution to the author(s), title of the work, publisher, and DOI.

Following irradiation, the activation detectors were removed from the chamber, and the energy spectra of photons from radionuclides generated from reactions of ^{209}Bi(n,xn)$^{210-x}$Bi(x=4-10), ^{12}C(n,2n)^{11}C and ^{27}Al(n,α)^{24}Na were measured using a high-purity germanium semiconductor detector (Ge-detector). Photo-peak counts were obtained for the corresponding photon energies. Table 1 gives the analysed radionuclide production reactions, half-lives and photon energies.

Photo-peak efficiencies of the Ge-detector, considering the self-absorption in the comparatively thick activation detectors, were estimated by simulations of electrons and photons using the MCNP5 Monte Carlo code [4]. The uncertainty of the efficiencies was estimated as approximately 5% due to the maximum discrepancy between the measurements and the simulations using a standard mixed-radionuclide point-source placed behind the non-irradiated samples of the activation detector.

Finally, the production rates (#/atm/U) of the radionuclide (#) per unit atom (atm) of the sample detectors per uranium beam particle (U) were estimated by considering the detector efficiencies and the beam intensity fluctuation during irradiation.

SIMULATION

Using the Particle and Heavy Ions Transport code System (PHITS) Ver-2.64 [5], a Monte Carlo simulation was performed using a model describing the experiment setup and the beam irradiation condition. The quantum molecular dynamics model JQMD [6] for heavy ion reactions and the intra-nuclear cascade model INCL [7] for neutrons above 20 MeV and protons were used as nuclear models in the simulation. For neutrons below 20 MeV, the JENDL-4.0 data library [8] was used.

Neutron and proton fluxes were estimated by track-length detector tallies of a half ring shape for 60 and 70 degrees and of a disk shape for 90 degrees as shown in Fig. 3. The ring-shape areas in the simulation for 60 and 70 degrees were made only under the beam line height symmetrical to the beam axis to obtain good statistics. Spectral differences between the positions in each half-ring region were found to be negligible.

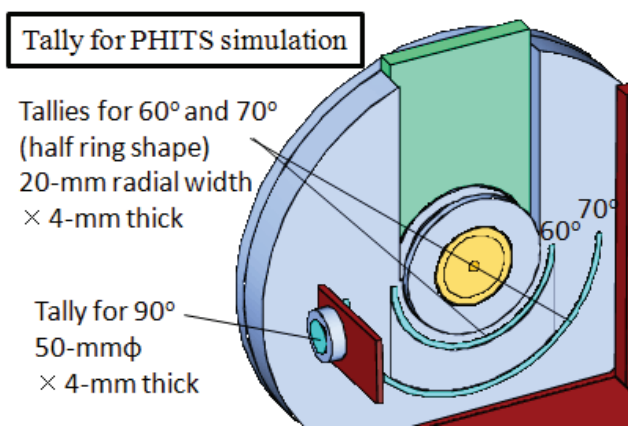

Figure 3: Detector tallies used in the PHITS simulations.

Table 1: Production Reactions, Half Lives and Photon Energies of the Radionuclides in the Activation Detectors

Reaction	Half life	Photon Energy (keV)
^{12}C(n,2n)^{11}C	20.4 min.	511
^{27}Al(n,α)^{24}Na	14.96 hr.	1369
^{209}Bi(n,4n)^{206}Bi	6.24 day	803.1, 881.0, 1718.7
^{209}Bi(n,5n)^{205}Bi	15.31 day	703.4, 1764.4
^{209}Bi(n,6n)^{204}Bi	11.22 hr.	899.2, 984.0
^{209}Bi(n,7n)^{203}Bi	11.76 hr.	820.2, 825.3, 1847.4
^{209}Bi(n,8n)^{202}Bi	1.72 hr.	422.2, 657.5, 960.7
^{209}Bi(n,9n)^{201}Bi	108 min.	629.1
^{209}Bi(n,10n)^{200}Bi	36.4 min.	419.7, 462.3, 1026.5

RESULTS AND DISCUSSION

The simulated energy spectra of neutrons and protons are shown in Fig. 4. Proton contributions to the activation reactions in the samples are negligible, as proton fluxes are much lower than those of neutrons. Production rates of the radionuclides were obtained by combining the simulated energy spectra of neutrons with the cross sections of the activation reactions shown in Fig. 5. The cross section for carbon was cited from JENDL/HE-2007 [9]. For aluminum and bismuth, cross sections evaluated by Maekawa et al. [10] were used.

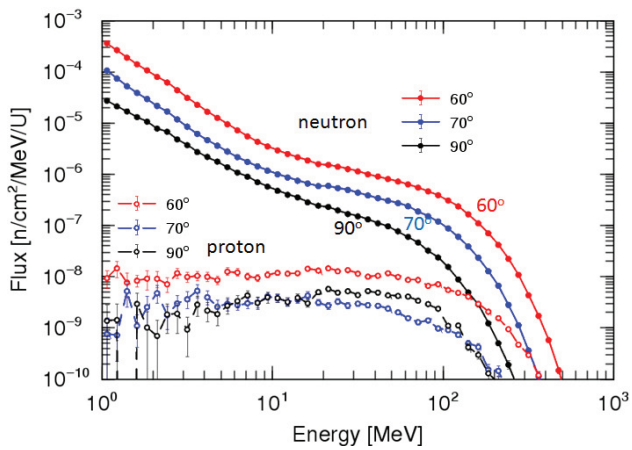

Figure 4: Energy spectra of neutrons and protons at the three activation detector locations.

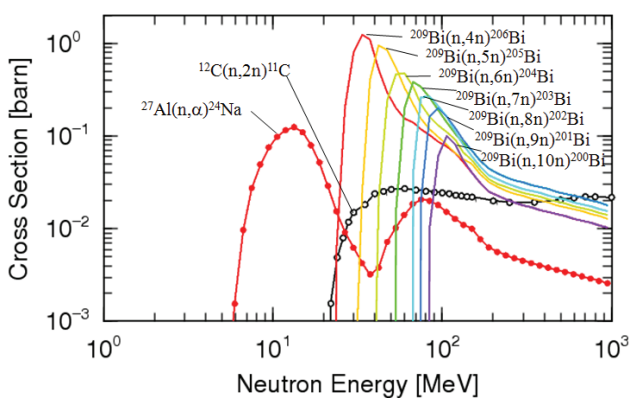

Figure 5: Cross sections of the activation reactions.

ISBN: 978-3-95450-132-8 doi:10.18429/JACoW-IPAC2014-TUPRI101

The measured and calculated radionuclide production rates were compared and some of the results are presented in Fig. 6. Differences between the 'side' and 'under' locations in the measured results at 60 degrees are most likely due to the difference between the upper and lower shield structures; however, further analysis is required to confirm this hypothesis.

Ratios of the calculated results to the experimental results are shown in Fig. 7 as a function of the peak energy of the cross section, which corresponds to the most sensitive energy for the reaction. For the carbon reaction, the threshold energy was used in this figure because the cross section was approximately constant above the threshold energy. Errors of the ratios range from 20 to 24% mainly due to the error of the beam intensity monitor. The ratios shown in the figure suggest that the simulated angular distribution of neutrons produced by ^{238}U irradiation on the beryllium target generally agreed with the experimental results from 10 to 100 MeV at 60, 70, and 90°. Additionally, for the neutron production, the energy dependence of the ratio of the calculated rates to the experimentally obtained rates was successfully determined by activation using bismuth, which has sensitive energies increasing about 10 MeV step as shown in Fig. 5.

Discrepancies are within a few % for the ^{27}Al(n,α) reaction and at a maximum of approximately 30% at the '60° side' and '70°' for the ^{12}C(n,2n) reaction. Overestimation of the calculations can be seen above 90 MeV for the '60° side' and '70°'. On the other hand, calculations for '60° under' and '90°' generally showed underestimations. The maximum discrepancy is approximately 60% at the '60° side' for the ^{209}Bi(n,10n) reaction. However, generally good agreements are seen between the measurements and simulations.

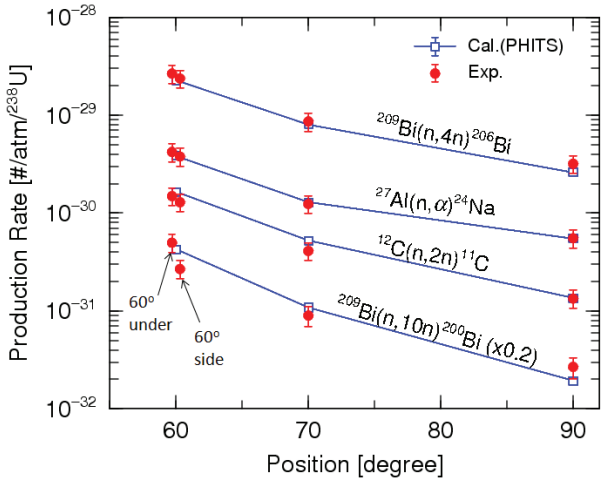

Figure 6: Production rates of several radionuclides.

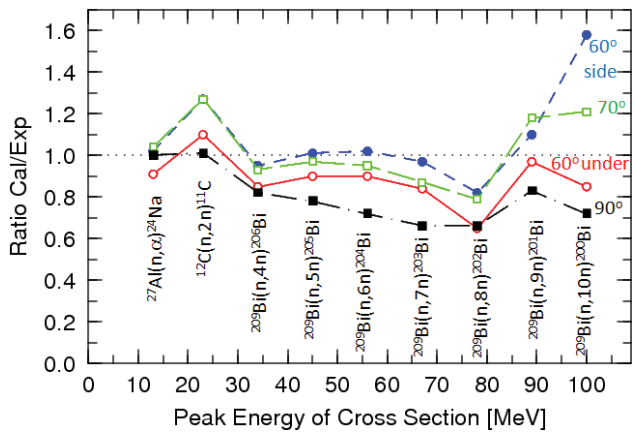

Figure 7: Ratio of the calculated production rates to the experiments as a function of the peak energy of the reaction cross sections (threshold energy for carbon).

CONCLUSION

Secondary neutrons from a target bombarded by a 345 MeV/u uranium beam were measured outside the target chamber using activation detectors, producing good benchmark experimental data. Comparisons with the PHITS simulation showed good agreements to within approximately 60%.

ACKNOWLEDGMENT

The authors are deeply grateful to the accelerator operation staff, the radiation safety office and the experimental groups at the RIBF for their helpful support in the parasitic experiment, and are also grateful to the RIKEN integrated Clusters facility group for their support in the calculation.

REFERENCES

[1] O. Yordanov et al., Nucl. Instr. and Meth. B 240 (2005) 863.
[2] Y. Yano et al., Nucl. Instr. and Meth. B 261 (2007) 1009.
[3] Y. Uwamino et al., "Secondary Radiation Measurement at BigRIPS of RIKEN RIBF", Proc. 10th Specialists' Meeting on Shielding Aspects of Accelerators, Targets and Irradiation Facilities (SATIF-10), Geneva, Switzerland, 2-7 June 2010.
[4] RSICC, Data Libraries for MCNP5, CCC-710/ MCNP, Oak Ridge National Laboratory (ORNL) (2003).
[5] T. Sato et al., J. Nucl. Sci. Technol. 50:9, 913-923 (2013).
[6] K. Niita et al., Phys. Rev. C 52, 2620 (1995).
[7] A. Boudard et al., Phys. Rev. C 87, 014606 (2013).
[8] K. Shibata et al,: "JENDL-4.0: A New Library for Nuclear Science and Engineering," *J. Nucl. Sci. Technol.* **48**(1), 1-30 (2011).
[9] H. Takada et al., J. Nucl. Sci. Technol., 46:6, 589–598 (2009).
[10] F. Maekawa et al., "Production of a Dosimetry Cross Section Set Up to 50 MeV", Proc. 10th International Symposium on Reactor Dosimetry, Sep. 12-17, 1999, Osaka, Japan p.417, American Society for Testing and Materials (2001).

Content from this work may be used under the terms of the CC BY 3.0 licence (© 2014). Any distribution of this work must maintain attribution to the author(s), title of the work, publisher, and DOI.